IEEE Access
Multidisciplinary ⋮ Rapid Review ⋮ Open Access Journal

Received 8 December 2022, accepted 16 January 2023, date of publication 19 January 2023, date of current version 25 January 2023.

Digital Object Identifier 10.1109/ACCESS.2023.3238100

RESEARCH ARTICLE

Underwater Acoustic Channel Estimation Based on Sparse Bayesian Learning Algorithm

SHUYANG JIA[1,2], SICHEN ZOU[2], XIAOCHUAN ZHANG[1,2], AND LIANGLONG DA[1,2]

[1]Naval Submarine Academy, Qingdao 266199, China
[2]Pilot National Laboratory for Marine Science and Technology, Qingdao 266237, China

Corresponding author: Sichen Zou (sichenzou1@163.com)

This work was supported in part by the National Key Research and Development Plan under Grant 2021YFC3100900, in part by the Qingdao National Laboratory of Marine Science and Technology under Grant 2021WHZZB0600, and in part by the Innovation Plan of Qingdao Collaborative Innovation Institute under Grant LYY-2022-05.

ABSTRACT The channel estimation algorithm based on sparse Bayesian learning proposed in recent years shows better performance than the traditional channel estimation algorithm by effectively reducing the convergence error in the channel estimation process. However, the sparse Bayesian learning algorithm based on expectation maximization (EM-SBL) is difficult to meet the practical applications with low complexity and power consumption. In order to guarantee the long-term stable communication of underwater devices, this paper proposes the fast sparse Bayesian learning algorithm based on Fast Marginal Likelihood Maximization (FM-SBL) to estimate underwater acoustic channels with low power consumption and high performance. Simulation and sea trial results show the output BER after channel estimation of FM-SBL is similar to that of EM-SBL, better than LS, MP and OMP, and it has good robustness in fast and slow time-varying channels. In terms of running speed, the FM-SBL algorithm is 16.7% of EM-SBL algorithm, which greatly reduces the estimation time.

INDEX TERMS Time-varying UWA channels, sparse Bayesian learning, channel estimation, robustness, complexity.

I. INTRODUCTION

Orthogonal frequency division multiplexing (OFDM), as a multicarrier modulation technique, has a wide range of applications in underwater acoustic (UWA) communication [1], [2], [3]. Due to high utilization of the frequency band, it is sensitive to symbol interference and subcarrier interference. Therefore, estimating the channel with an efficient and accurate way is very important.

To begin with, the least square (LS) method for channel estimation was first widely used [4]. In recent years, along with the sparsity of UWA channels being exploited, Compressed Sensing (CS) algorithm has been studied and applied as a common channel estimation method [5], [6], [7], [8]. Paper [9], [10], [11] achieved better channel estimation performance by Orthogonal Matching Pursuit (OMP) and Basis Pursuit (BP) algorithms to estimate both path delay and path Doppler scale, but the calculation is higher than LS algorithm. The paper [12] proposed a bidirectional channel estimation scheme with low computational complexity, while the number of pilot symbols required is very large. With the development of artificial intelligence techniques, channel estimation algorithms based on neural network have also emerged [13], [14], [15]. The paper [16] formulated channel estimation as a sparse signal recovery problem and implemented through classical iterative algorithms approximate message passing (AMP), however, these existing schemes do not achieve satisfactory estimation accuracy. In recent years, some channel estimation schemes based on sparse Bayesian learning have been proposed. The paper [17], [18], [19], [20] investigated channel estimation based on a sparse Bayesian learning framework, which has the desirable property of preventing convergence errors by exploiting the sparsity of the channel in the time delay and Doppler direction, resulting in more accurate channel estimation and making the output BER lower compared to the CS approach. However, because the

The associate editor coordinating the review of this manuscript and approving it for publication was Marco Martalo.

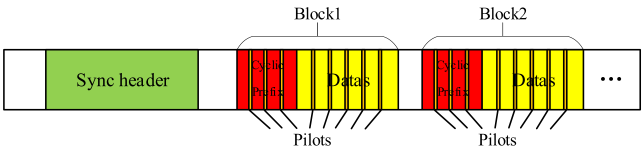

FIGURE 1. **The structure of one frame OFDM signal.**

algorithm is based on the expectation-maximization iterative algorithm with high complexity, it consumes long time and large power consumption to obtain better performance. Especially in OFDM communication, there are multiple blocks to estimate in one frame, which is completely unable to meet the practical application of underwater communication devices. Therefore, it is necessary to obtain an algorithm with relatively high computational accuracy and low complexity to guarantee the large-scale long-time communication applications [21], [22].

In OFDM communication, a frame signal contains multiple OFDM blocks. Each block needs to be estimated and demodulated individually. The cycle prefixes are in the front of the blocks to prevent symbol interference. Pilots are inserted into each block at equal intervals. The specific frame structure is shown in FIGURE 1. Due to the high band frequency utilization and fast communication efficiency of OFDM, the time interval between blocks is very short. In order to fully save the time of OFDM communication and keep the reception normal, the hardware is required to complete a series of processing operations such as channel estimation and decoding algorithm of the last signal block synchronously within the time of receiving a signal block. Otherwise, if the processing time exceeds the time to receive a signal block, it will lead to a continuous accumulation of signals, which not only occupies the chip memory, but also does not guarantee the timeliness of OFDM communication and wastes the advantages of high-speed transmission of OFDM communication. Because OFDM uses LDPC decoding, in order to improve the correct rate of decoding, the decoding algorithm generally requires multiple iterations, thus taking up most of the back-end processing time. In previous applications, high performance and low complexity cannot be achieved at the same time, and in order to leave sufficient time for the decoding algorithm, the LS algorithm with lower estimation performance is often used for channel estimation.

The FMLM is first given in [23]. The paper [24] uses FMLM to update the definition set, which is feasible to handle large-scale data in an inductive manner. In order to obtain an algorithm with relatively high computational accuracy and low complexity to guarantee the large-scale long-term communication capability of underwater devices, this paper uses FMLM and Woodbury decomposition of the cost function to obtain a low-complexity parametric update algorithm [25], [26].

This paper focuses on a low-complexity and efficient channel estimation algorithm for UWA OFDM communication. In Section II, the OFDM system and channel model are introduced. In Section III, The EM-SBL algorithm and the FM-SBL channel estimation algorithm are introduced in detail, respectively. Then algorithmic complexity is analyzed and compared. Section IV gives the parameter settings and verifies the channel estimation results comparison of different algorithms in the simulation and experiment. The conclusions are shown in Section V.

II. SYSTEM MODEL

In this section, we present the OFDM system and UWA channel model.

A. OFDM SYSTEM

Assuming that the number of subcarriers of the OFDM system is K, the bandwidth is B, and the lowest subcarrier frequency is f_l. The subcarrier frequency interval is $\Delta f = B/K$, and the frequency of the kth subcarrier can be expressed as

$$f_k = f_l + k\Delta f \quad k = 0, \cdots K-1. \tag{1}$$

The time domain signal $x(t)$ can be expressed as

$$x(t) = 2Re\left\{\sum_{k=-K/2}^{K/2-1} d_k e^{j2\pi f_k t}\right\} \; t \in [0, T]. \tag{2}$$

where $Re\{\cdot\}$ is taking the real part and dk is the symbol after QPSK modulation. $T = 1/\Delta f$ is denoted as the period of an OFDM symbol. After adding the cyclic prefix, $x(t)$ then passes through the channel.

Suppose there are M multipath UWA channels, N pilots in one OFDM block, and the $N \times 1$ received signal $\boldsymbol{Y}$ function is

$$\begin{aligned} \boldsymbol{Y}_{[N,1]} &= \boldsymbol{X}_{[N,N]}\tilde{\boldsymbol{H}}_{[N,1]} + \boldsymbol{E}_{[N,1]} \\ &= \boldsymbol{X}_{[N,N]}\boldsymbol{F}_{[N,M]}\boldsymbol{H}_{[M,1]} + \boldsymbol{E}_{[N,1]} \\ &= \boldsymbol{\Phi}_{[N,M]}\boldsymbol{H}_{[M,1]} + \boldsymbol{E}_{[N,1]}. \end{aligned} \tag{3}$$

where $\boldsymbol{X}$ is the $N \times N$transmitted signal stored in a diagonal matrix, $\boldsymbol{F}$ is a $N \times M$Fourier transform matrix, and their product is denoted as $\boldsymbol{\Phi}$. $\tilde{\boldsymbol{H}}$ represents the channel function in frequency domain, while $\boldsymbol{H}$ represents the channel impulse response in time domain. $\boldsymbol{E}$ is additive noise, which obeys Gaussian distribution with the mean of zero and variance σ^2, which can be obtained from the square of the empty carrier. For the sake of description, subscripts that indicate the dimension of matrix are omitted below.

The method of self-correlators for CP is adopted to estimate the Doppler scales block-by-block. Then the received data is resampled with estimated Doppler factor. The dominating Doppler effects are considered to be compensated and the residual are considered as additive noise.

B. CHANNEL MODEL

The $\boldsymbol{H}$ is divided into Msegments as show in (4). The length of the mth segment channel $\boldsymbol{h}_m$ which obeys a Gaussian distribution with a mean of 0 and variance γ_m. When γ_m is small enough, the amplitude of this channel segment is almost 0. Therefore, it is most likely to be a noise. Overall, the channel is relatively sparse because most channel segments are noise. FIGURE 7 in section IV can also show this phenomenon.

$$\boldsymbol{H} = [\underbrace{h_1, \cdots, h_{d_1}}_{\boldsymbol{h}_1}, \cdots, \underbrace{h_1, \cdots, h_{d_M}}_{\boldsymbol{h}_M}] \tag{4}$$

The distribution of $\boldsymbol{H}$ can be as follows.

$$p(\boldsymbol{H}) \sim \mathcal{CN}(0, \boldsymbol{\Gamma}) \tag{5}$$

where $\boldsymbol{\Gamma}$ is the diagonal matrix of γ_m that controls the variance of the channel, which is one of the parameters of the request.

$$\boldsymbol{\Gamma}=\text{diag}([\gamma_1 \cdots \gamma_m \cdots \gamma_M]) \tag{6}$$

III. CHANNEL ESTIMATION ALGORITHM

In this section, the EM-SBL and FM-SBL algorithms for channel estimation are investigated, which are fundamentally two different calculating methods of the cost function.

A. EM-SBL

The EM-SBL algorithm is based on expectation maximization, where the hyperparameters are updated alternately by expectation and maximization during the iterative process. These hyperparameters can be estimated using a type II maximum likelihood function, which maximizes the posterior probability distribution function $\mathrm{p}(\boldsymbol{H}|\boldsymbol{Y}; \boldsymbol{\Gamma})$ because it is difficult to find $\boldsymbol{\Gamma}$ in $\mathrm{p}(\boldsymbol{H}; \boldsymbol{\Gamma})$.

For the pilot signal $\boldsymbol{Y}$ received after passing through the channel, it obeys the following probability density distribution.

$$\begin{aligned} p(\boldsymbol{Y}|\boldsymbol{H}) &\sim \mathcal{CN}(\boldsymbol{\Phi H}, \sigma^2 \boldsymbol{I}) \\ &= (2\pi\sigma^2\boldsymbol{I})^{-\frac{N}{2}} \exp\left(-\frac{(\boldsymbol{Y}-\boldsymbol{\Phi H})^{\mathrm{H}}(\boldsymbol{Y}-\boldsymbol{\Phi H})}{2\sigma^2 \boldsymbol{I}}\right) \end{aligned} \tag{7}$$

Combined with Bayesian equations and Gaussian constant equations in Appendix D of P. R. Mahler's book [27](the proof in Bar-Shalom's book [28]). We get

$$\mathrm{p}(\boldsymbol{Y}|\boldsymbol{H})\mathrm{p}(\boldsymbol{H}; \boldsymbol{\Gamma}) = \mathrm{p}(\boldsymbol{H}|\boldsymbol{Y}; \boldsymbol{\Gamma})\mathrm{p}(\boldsymbol{Y}). \tag{8}$$

And the distribution of $\mathrm{p}(\boldsymbol{H}|\boldsymbol{Y}; \boldsymbol{\Gamma})$, $\mathrm{p}(\boldsymbol{Y}; \boldsymbol{\Gamma})$are

$$\begin{aligned} p(\boldsymbol{H}|\boldsymbol{Y}; \boldsymbol{\Gamma}) &\sim \mathcal{CN}(\boldsymbol{M}, \boldsymbol{\Sigma}) \\ p(\boldsymbol{Y}; \boldsymbol{\Gamma}) &\sim \mathcal{CN}(\boldsymbol{0}, \boldsymbol{C}). \end{aligned} \tag{9}$$

where the parameters corresponding to (9) are

$$\begin{aligned} \boldsymbol{M} &= \sigma^2 \boldsymbol{\Sigma} \boldsymbol{\Phi}^{\mathrm{H}} \boldsymbol{Y} \\ \boldsymbol{\Sigma} &= (\boldsymbol{\Gamma}^{-1} + \sigma^2 \boldsymbol{\Phi}^{\mathrm{H}} \boldsymbol{\Phi})^{-1} \\ \boldsymbol{C} &= \sigma^{-2}\boldsymbol{I} + \boldsymbol{\Phi\Gamma\Phi}^{\mathrm{H}}. \end{aligned} \tag{10}$$

The EM algorithm consists of two steps, step E and step M. The step E is

$$\begin{aligned} \boldsymbol{\Gamma}^{j+1} &= \arg\max_{\boldsymbol{\Gamma}} \mathrm{E}_{\boldsymbol{H}/Y, \boldsymbol{\Gamma}^j} \left[\ln \mathrm{p}(\boldsymbol{H}; \boldsymbol{\Gamma})\right] \\ &= \mathrm{E}_{\boldsymbol{H}/Y, \boldsymbol{\Gamma}^j} \boldsymbol{H}^2 \\ &= \boldsymbol{M}\boldsymbol{M}^{\mathrm{H}} + \boldsymbol{\Sigma}. \end{aligned} \tag{11}$$

Bring $\boldsymbol{M}$, $\boldsymbol{\Sigma}$ in (10) into (11). The parameters $\boldsymbol{\Gamma}$ are constantly updated to be stable during iteration [29].

The estimated channel $\hat{\boldsymbol{H}}$ is $\mathbf{M}$, i.e., $\hat{\boldsymbol{H}} = \mathbf{M}$. The flow of EM-SBL algorithm is shown in Algorithm 1.

Algorithm 1 EM-SBL Channel Estimation Procedure

Initialization:

Set σ^2=E$(\mathbf{Y}_{empt})^2$, $\boldsymbol{Y}$, $\boldsymbol{\Phi}$, $\boldsymbol{\Gamma} = \boldsymbol{I}$, $iterMax$, th

While ($i < iterMax$ &$|\Gamma_{(i+1)} - \Gamma_{(i)}|/\Gamma_{(i)} > th$) do

Calculate $\boldsymbol{\Sigma} = (\boldsymbol{\Gamma}_{(i)}^{-1} + \sigma^2\boldsymbol{\Phi}^{\mathrm{H}}\boldsymbol{\Phi})^{-1}$, $\boldsymbol{M} = \sigma^2\boldsymbol{\Sigma}\boldsymbol{\Phi}^{\mathrm{H}}\boldsymbol{Y}$

Calculate $\boldsymbol{\Gamma}_{(i+1)} = \boldsymbol{M}\boldsymbol{M}^{\mathrm{H}} + \boldsymbol{\Sigma}$

End while

Output $\mathbf{M}$, $\boldsymbol{\Gamma}_{(i+1)}$

B. FM-SBL

Unlike the EM algorithm, the FM-SBL algorithm uses $\mathrm{p}(\boldsymbol{Y})$ as the cost function.

$$\begin{aligned} l(\boldsymbol{\Gamma}) &= -2\ln \mathrm{p}(\boldsymbol{Y}) \\ &= -2\ln\left\{\frac{1}{\sqrt{2\pi}}\boldsymbol{C}^{-1/2}\exp\left(-\frac{1}{2}\boldsymbol{Y}^H\boldsymbol{C}^{-1}\boldsymbol{Y}\right)\right\} \\ &= \ln|\boldsymbol{C}| + \boldsymbol{Y}^H\boldsymbol{C}^{-1}\boldsymbol{Y} + \ln 2\pi. \end{aligned} \tag{12}$$

Ignore the constant term. Now use Woodbury decomposition [23] to further analyze $\boldsymbol{C}$ in (10). Since the $\boldsymbol{\Gamma}$ is diagonal matrix, rewrite $\boldsymbol{C}$ as

$$\begin{aligned} \boldsymbol{C} &= \sigma^{-2}\boldsymbol{I} + \boldsymbol{\Phi\Gamma\Phi}^{\mathrm{H}} \\ &= \sigma^{-2}\boldsymbol{I} + \sum_{j\neq i}\boldsymbol{\Phi}_j\boldsymbol{\Gamma}_{jj}\boldsymbol{\Phi}_j^{\mathrm{H}} + \boldsymbol{\Phi}_i\boldsymbol{\Gamma}_{ii}\boldsymbol{\Phi}_i^{\mathrm{H}} \\ &= \boldsymbol{C}_{-i} + \boldsymbol{\Phi}_i\boldsymbol{\Gamma}_{ii}\boldsymbol{\Phi}_i^{\mathrm{H}}. \\ &= \boldsymbol{C}_{-i} + \gamma_i\boldsymbol{\Phi}_i\boldsymbol{\Phi}_i^{\mathrm{H}} \end{aligned} \tag{13}$$

where the $N \times 1$ vector $\boldsymbol{\Phi}_i$ is the ith column of $\boldsymbol{\Phi}$. $\boldsymbol{C}_{-i} = \sigma^{-2}\boldsymbol{I} + \sum_{j\neq i}\boldsymbol{\Phi}_j\boldsymbol{\Gamma}_{jj}\boldsymbol{\Phi}_j^{\mathrm{H}}$ is a $N \times N$ matrix. $\boldsymbol{\Gamma}_{ii} = \gamma_i$ is the ith row and ith column of $\boldsymbol{\Gamma}$. The Matrix Inversion Lemma also called Sherman-Morrison-Woodbury theory is used to get $|\boldsymbol{C}|$ and $\boldsymbol{C}^{-1}$ [23].

$$\begin{aligned} |\mathbf{C}| &= |1 + s_i\gamma_i|\,|\mathbf{C}_{-i}| \\ \mathbf{C}^{-1} &= \mathbf{C}_{-i}^{-1} - \gamma_i(1 + s_i\gamma_i)^{-1}\mathbf{C}_{-i}^{-1}\boldsymbol{\Phi}_i\boldsymbol{\Phi}_i^{\mathrm{H}}\mathbf{C}_{-i}^{-1} \end{aligned} \tag{14}$$

Define $s_i = \boldsymbol{\Phi}_i^{\mathrm{H}}\boldsymbol{C}_{-i}^{-1}\boldsymbol{\Phi}_i$, $q_i = \boldsymbol{\Phi}_i^{\mathrm{H}}\boldsymbol{C}_{-i}^{-1}\boldsymbol{Y}$. The s_i and q_i are both two numbers. According to (14), splitting the cost function, we get

$$\begin{aligned} \mathcal{L} &= \ln|\boldsymbol{C}_{-i}| + \mathbf{Y}^{\mathrm{H}}\boldsymbol{C}_{-i}^{-1}\mathbf{Y} + \ln|1 + \gamma_i s_i| - q_i^2(\gamma_i^{-1} + s_i)^{-1} \\ &= \mathcal{L}(-i) + \mathcal{L}(i). \end{aligned} \tag{15}$$

where $\mathcal{L}(i) = \ln|1 + \gamma_i s_i| - q_i^2(\gamma_i^{-1} + s_i)^{-1}$, the rest is $\mathcal{L}(-i)$. Because $\mathcal{L}(-i)$ does not contain the information of γ_i. Therefore, $\partial\mathcal{L}(i)/\partial\gamma_i = 0$ is solved to get γ_i. Then γ_i is restored to a diagonal array $\boldsymbol{\Gamma}$. $\boldsymbol{M}$ and $\boldsymbol{\Sigma}$ are easily calculated by (10).

$$\boldsymbol{\Gamma}=\text{diag}(\gamma_i) = \text{diag}(s_i^{-1}(q_i^2 s_i^{-1} - 1)) \; i = 1 \cdots M \quad (16)$$

In practice, for most of the cases, the UWA channel exhibits strong temporal correlation over a time scale less than the channel coherence time. Therefore, to accelerate convergence speed, the $\boldsymbol{\Gamma}$ of the previous block can be used when initializing the second block.

The procedure of FM-SBL is given below.

Algorithm 2 FM-SBL Channel Estimation Procedure

Initialization:

Set σ^2=E$(\mathbf{Y}_{empt})^2$, $\boldsymbol{Y}$, $\boldsymbol{\Phi}$, $\boldsymbol{\Gamma} = \boldsymbol{I}$, $iterMax$, th

While(k <$iterMax$ &$|\tilde{\boldsymbol{A}}_{(k+1)}$ -$\tilde{\boldsymbol{A}}_{(k)}|/\tilde{\boldsymbol{A}}_{(k)}$ >th) do

For (i=1, $i <= M$, $i++$)

$$\boldsymbol{C}_{-i} = \sigma^{-2}\boldsymbol{I} + \sum_{j \neq i} \boldsymbol{\Phi}_j \boldsymbol{\Gamma}_{jj} \boldsymbol{\Phi}_j^{\text{H}}$$

Calculate $s_i = \boldsymbol{\Phi}_i^{\text{H}} \boldsymbol{C}_{-i}^{-1} \boldsymbol{\Phi}_i$

$q_i = \boldsymbol{\Phi}_i^{\text{H}} \boldsymbol{C}_{-i}^{-1} \boldsymbol{Y}$

$\gamma_i = s_i^{-1}(q_i^2 s_i^{-1} - 1)$

End For

$\boldsymbol{\Gamma}_{(k+1)}$=diag$(\gamma_i)$ $\; i = 1 \cdots M$

End While

Calculate $\boldsymbol{\Sigma} = (\boldsymbol{\Gamma}_{(k+1)}^{-1} + \sigma^2 \boldsymbol{\Phi}^{\text{H}} \boldsymbol{\Phi})^{-1}$

$\boldsymbol{M} = \sigma^2 \boldsymbol{\Sigma} \boldsymbol{\Phi}^{\text{H}} \boldsymbol{Y}$

Output $\hat{\boldsymbol{H}} = \mathbf{M}, \boldsymbol{\Gamma}$

C. ALGORITHM COMPLEXITY ANALYSIS

The computational complexity of each iteration between the EM-SBL algorithm and FM-SBL proposed in this paper are discussed.

For EM-SBL algorithm, the main calculation quantities are estimating $\boldsymbol{\Sigma}$,$\boldsymbol{M}$ and updating $\boldsymbol{\Gamma}$.Where, the complexity of $\boldsymbol{\Sigma}$ is $\mathcal{O}(M^3)$, the complexity of $\boldsymbol{M}$ is $\mathcal{O}(M^2N)$, and the complexity of $\boldsymbol{\Gamma}$ is $\mathcal{O}(M)$. In summary, because $M < N$, the complexity of the EM–SBL algorithm is $\mathcal{O}(M^2N)$ in each iteration.

While for FM-SBL algorithm, owing to Woodbury decomposition and FMLM optimization methods, its computational efficiency can be greatly improved. Choose the *ith* column, the complexity of solving $\boldsymbol{C}_{-i}$ is $\mathcal{O}(M)$. Since $\boldsymbol{\Gamma}$=diag$(\gamma_1 \cdots \gamma_i \cdots \gamma_M)$, the properties of diagonal matrices can be utilized to reduce the calculation. It is sufficient to converge $\boldsymbol{\Gamma}$ to a stable value. The complexity of solving $\boldsymbol{\Gamma}$ in each iteration is $\mathcal{O}(M^2)$.

IV. EXPERIMENTS AND ANALYSIS

The process of an UWA OFDM communication system is shown in FIGURE 2. The performance of the algorithm is demonstrated and analyzed by simulation and sea trial data respectively. The robustness of the algorithm is simulated by fast time-varying channel and slow time-varying channel, and the performance evaluation indexes include the bit error rate (BER) and channel mean square error (MSE), the time and power consumption and so on.

A. NUMERICAL SIMULATION AND ANALYSIS

The simulated signal contains 4 OFDM blocks per frame, each OFDM block has $N = 256$ subcarriers, of which, $N_d = 192$ data subcarriers and $N_p = 64$pilot subcarriers, and the coding method is LDPC coding with code rate of 1/2, and the modulation method is QPSK modulation. The sampling frequency is $f_s = 12$kHz, the inserted pilot interval is 4, the center frequency after up conversion is $f_c = 2.25$kHz, and the bandwidth is $B = 1.5$kHz.

The analog UWA channels simulate the main characteristics of oceanic channels on slow time-varying channels and fast time-varying channels respectively. The simulation randomly generates 10 channels with delay variation of [0,0.5]ms and gain amplitude variation of [0.5,1.5] for the fast time-varying channel. For the slow time-varying channel, the delay variation is randomly selected in [0,0.1]ms and the gain amplitude variation range is randomly selected in [0.8,1.2]. The Doppler factor ranges from -2e-4 to 1e-4, the amplitude obeys Rayleigh distribution, and the average power decreases exponentially at any time delay. Algorithms simulated in FIGURE 3 are single-tap channel estimation algorithms (LS-line, LS-spline) and CS based algorithms (MP, OMP, EM-SBL, FM-SBL).

The performance evaluation metrics are the simulation results of the output BER, channel mean square error and the time consumption with SNR and pilot numbers. Where, the runtime is obtained by tic-toc command of MATLAB.

The theoretical value and several channel estimation curves are studied and their performance is compared, where the theoretical value curves are affected only by the SNR and rather than the Doppler channel. From FIGURE 3 (a) and (b), it can be seen that all BER and channel MSE keep decreasing with the increase of SNR. Among them, LS algorithm has the worst performance, MP and OMP algorithms are the next best, and EM-SBL and FM-SBL algorithms have the best results and are closest to the theoretical values. Since the EM-SBL algorithm uses an iterative algorithm based on expectation maximization, the optimal channel estimation results can be obtained. However, under the condition of almost the same BER, the calculation speed of the FM-SBL algorithm is significantly faster than that of the EM-SBL algorithm.

The simulation performance in FIGURE 4 has an overall similar trend to FIGURE 3. The comparison between FIGURE 3 and FIGURE 4 reveals that the BER and MSE

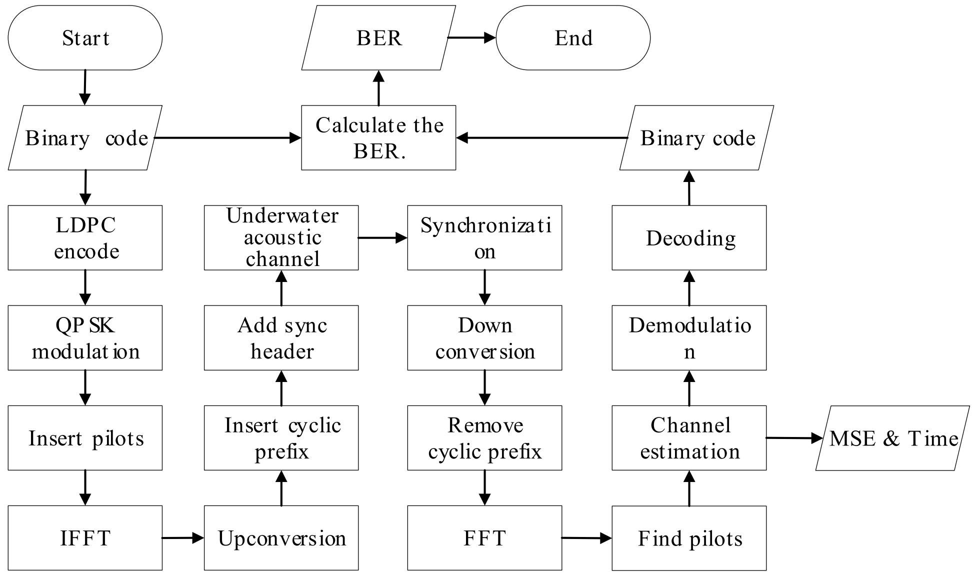

FIGURE 2. **The UWA OFDM communication flow char.**

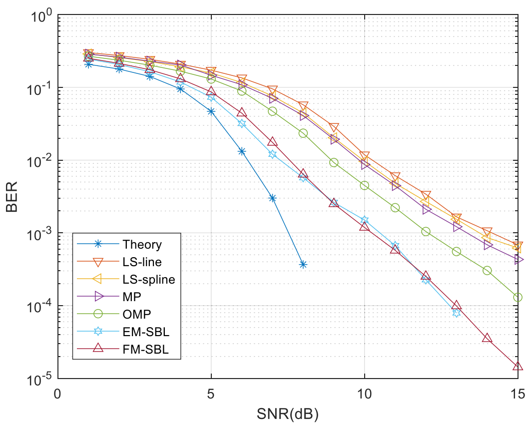

(a) BER in slow time-varying channel.

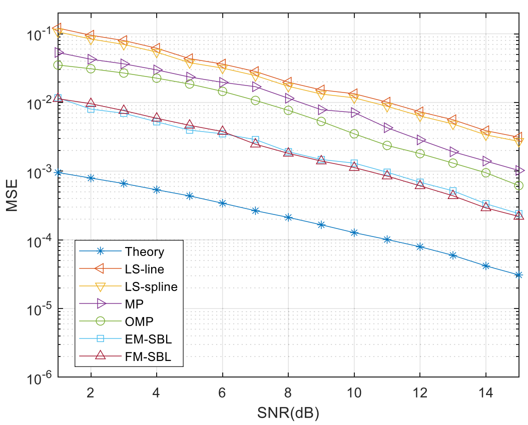

(b) MSE in slow time-varying channel.

FIGURE 3. **The simulation performance comparison in slow time-varying channel.**

performance of channel estimation algorithms under fast time-varying channels is slightly less desirable than under slow time-varying channels. However, the performance of the SBL algorithm is still the best. The effectiveness and robustness of the algorithm is further verified by both slow and fast time-varying channel.

FIGURE 5 shows that the FM-SBL algorithm has a very high operational efficiency, and the average results of 1000 MATLAB simulations under the same condition settings are 1.27s for EM-SBL, while only 0.12s for FM-SBL. Secondly, by comparing the upper and lower horizontal variables, it is found that the time consumption required for channel estimation is insensitive to the change of SNR. As the SNR decreases, the time consumption is basically smooth and does not change much overall. While as the number of pilot N_p increases, the time consumption of each algorithm increases significantly. It is further found that the more the number of leads, the more obvious is the advantage of FM-SBL algorithm, which reflects the superiority of this algorithm in large-scale UWA communication applications.

B. SEA TRIAL EXPERIMENT AND ANALYSIS

The sea trial data were collected on November 24, 2021, in Qingdao sea, a water depth of 16.7 m. The sea trial tested the self-developed motherboard, as shown in FIGURE 6. The transmitter point was anchored with a depth of 5 m. The receiver sensor depth was 7 m. The transmitter and receiver points were separated by 3-5 nautical miles in increasing order. The sea wind was 3∼4 degrees. The wave height was 1∼1.5 m.

The transmission interval per frame is 1 second, with 8 OFDM blocks per frame. The channel is estimated block-by-block of OFDM in single frame. The parameters of the sea trial OFDM system are set differently from the simulation parameters, and some of them are shown in Table 1.

The channel is judged to be a fast or slow time-varying channel based on the different performance of each frame signal in terms of delay and gain. The evaluation metrics such

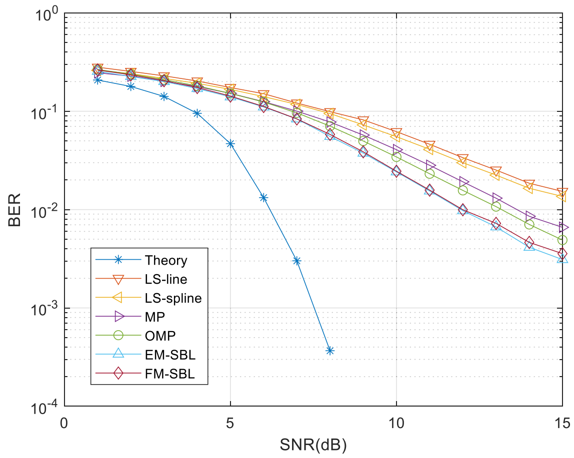

(a) BER in fast time-varying channel

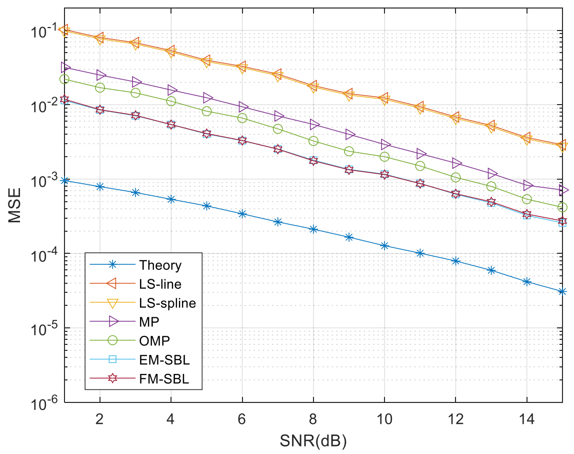

(b) MSE in fast time-varying channel.

FIGURE 4. **The simulation performance comparison in fast time-varying channel.**

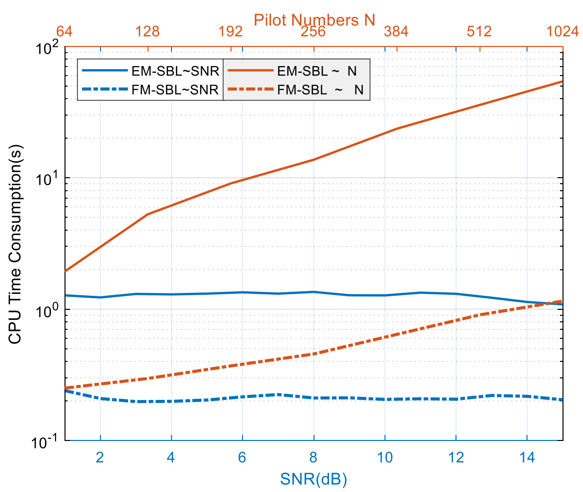

FIGURE 5. **Time consumption with SNR & pilot Numbers.**

as channel impulse response (CIR), channel delay offsets of blocks, bit error rate (BER) and hardware power consumption evaluation of the algorithm are given below.

FIGURE 6. **Hardware of UWA communication system.**

TABLE 1. **Parameters of OFDM UWA communication system.**

Bandwidth	Subcarrier spacing	Modulation mode	Signal length
6kHz	5.8594Hz	QPSK	256ms
Carrier frequency	**Sampling frequency**	**Pilot interval**	**Cyclic prefix**
11kHz	48kHz	3	42.67ms

FIGURE 7 shows the channel impulse response of 8 consecutive blocks in one frame. The channel impulse response estimated by each algorithm shows a relatively sparse characteristic with basically a number of stable and obvious multipaths from 0 to 7 ms, and the energy of multipaths is weaker and tends to 0 after 8 ms.

Define the delay offset between the *lth* block and the $(l+1)th$ block in *kth* frame data as

$$\tau_{offset}(k, l) = \tau(l+1) - \tau(l) \; k, l = 1 \cdots 7. \qquad (17)$$

The calculation results for the delay offsets of 7 frames are shown as FIGURE 8.

It can be seen from FIGURE 8 that in the fourth frame of sea trial data, the channel delay offsets between blocks are the largest, exceeding 0.4 ms. The channel delay offsets in the second frame and the seventh frame are next, and the rest are relatively small. Some points can be summarized that for frames (2, 4 and 7), the channels can be considered to be fast time-varying according to FIGURE 8, while the others can be inferred as slow time-varying channel.

FIGURE 9 is the BER performance comparison of three algorithms for seven frame sea trial data. The BER of EM-SBL and FM-SBL algorithm are almost close. Further analysis has been conducted on the data collected from the sea trial in Qingdao. No matter the fast or slow time-varying channel, the BER of EM-SBL and FM-SBL are both robust and better than that of OMP.

The hardware of the algorithm is implemented on a DSP by Code Composer Studio. Performance evaluation indicators include the clock cycle, the average power of hardware

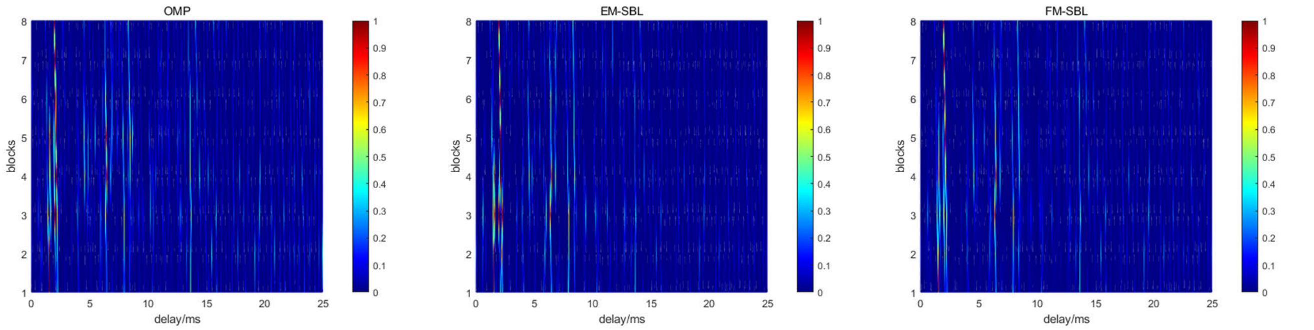

FIGURE 7. Performance comparison of CIR of one frame sea trial data.

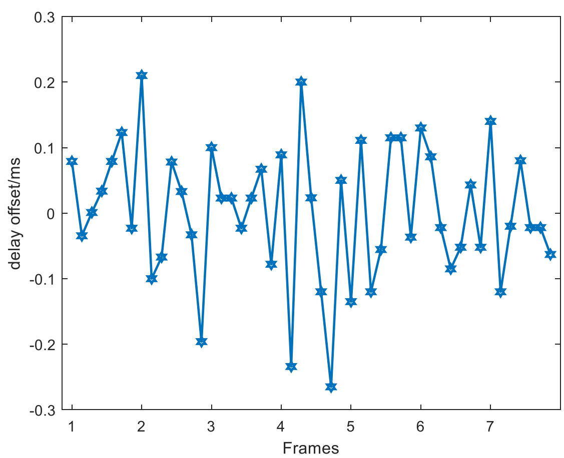

FIGURE 8. The delay offsets of 7 frames.

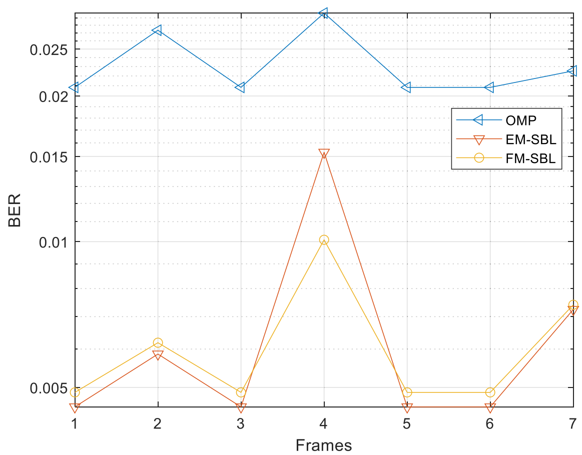

FIGURE 9. BER of 7 frames sea trial data.

operation, and the total power consumption. The clock period is recorded by the Time Samp Counter (TSC) on Code Composer Studio, the power of the hardware operation is measured by a DC regulated power supply and a digital multimeter, from which the total power consumption is calculated. The hardware utilization and power consumption are shown in Table 2. It can be seen that the FM-SBL algorithm requires less time and consumes only 16.67% of the time and power consumption of the SBL algorithm with similar average power.

TABLE 2. Hardware evaluation indicators.

Algorithm	Clock cycle	Power /mW	Total energy consumption /mJ
EM-SBL	75240000	199	0.33
FM-SBL	12541570	200	0.055

V. CONCLUSION

This paper discusses the performance and efficiency of channel estimation, and proposes a fast sparse Bayesian learning algorithm for underwater communication channel estimation. The FM-SBL algorithm improves the operation efficiency by 16.7% compared with EM-SBL algorithm. Meanwhile, it has more accurate channel estimation performance than LS, MP, OMP algorithms and the similar performance to that of EM-SBL. Simulation results show that the algorithm has good performance and strong robustness in time-varying channel estimation. In addition, experiment verifies hardware resources and chip power consumption are greatly reduced. The computational efficiency can be greatly improved, which is very suitable for energy-saving and large-scale underwater acoustic communication.

REFERENCES

[1] M. B. Mashhadi and D. Gunduz, "Pruning the pilots: Deep learning-based pilot design and channel estimation for MIMO-OFDM systems," *IEEE Trans. Wireless Commun.*, vol. 20, no. 10, pp. 6315–6328, Oct. 2021.

[2] S. Barua, Y. Rong, S. Nordholm, and P. Chen, "Adaptive modulation for underwater acoustic OFDM communication," in *Proc. OCEANS Marseille*, Jun. 2019, pp. 1–5.

[3] R. Jiang, S. Cao, C. Xue, and L. Tang, "Modeling and analyzing of underwater acoustic channels with curvilinear boundaries in shallow ocean," in *Proc. IEEE Int. Conf. Signal Process., Commun. Comput. (ICSPCC)*, Oct. 2017, pp. 1–6.

[4] S. J. Lee, "On the training of MIMO-OFDM channels with least square channel estimation and linear interpolation," *IEEE Commun. Lett.*, vol. 12, no. 2, pp. 100–102, Feb. 2008.

[5] C. Knill, B. Schweizer, S. Sparrer, F. Roos, R. F. H. Fischer, and C. Waldschmidt, "High range and Doppler resolution by application of compressed sensing using low baseband bandwidth OFDM radar," *IEEE Trans. Microw. Theory Techn.*, vol. 66, no. 7, pp. 3535–3546, Jul. 2018.

[6] S. Lu, I. A. Hemadeh, M. El-Hajjar, and L. Hanzo, "Compressed-sensing-aided space-time frequency index modulation," *IEEE Trans. Veh. Technol.*, vol. 67, no. 7, pp. 6259–6271, Jul. 2018.

[7] Y. Lin, K. Song, and M. S. Yun, "Iterative clipping noise recovery of OFDM signals based on compressed sensing," *IEEE Trans. Broadcast.*, vol. 63, no. 4, pp. 706–713, Dec. 2017.

[8] Y.-H. Zhou, F. Tong, and G. -Q. Zhang, "Distributed compressed sensing estimation of underwater acoustic OFDM channel," *Appl. Acoust.*, vol. 117, pp. 160–166, Feb. 2017.

[9] C. R. Berger, S. Zhou, J. C. Preisig, and P. Willett, "Sparse channel estimation for multicarrier underwater acoustic communication: From subspace methods to compressed sensing," *IEEE Trans. Signal Process.*, vol. 58, no. 3, pp. 1708–1721, Mar. 2010.

[10] M. A. Khojastepour, K. Gomadam, and X. Wang, "Pilot-assisted channel estimation for MIMO OFDM systems using theory of sparse signal recovery," in *Proc. IEEE Int. Conf. Acoust., Speech Signal Process.*, Apr. 2009, pp. 2693–2696.

[11] H.-N. Yu and S.-X. Guo, "Research on CS-based channel estimation methods for UWB communications," *J. Electron. Inf. Technol.*, vol. 34, no. 6, pp. 1452–1456, Aug. 2012.

[12] L. Yang, Y. Zeng, and R. Zhang, "Channel estimation for millimeter-wave MIMO communications with lens antenna arrays," *IEEE Trans. Veh. Technol.*, vol. 67, no. 4, pp. 3239–3251, Apr. 2018.

[13] W. Zhang, X. Yang, C. Leng, J. Wang, and S. Mao, "Modulation recognition of underwater acoustic signals using deep hybrid neural networks," *IEEE Trans. Wireless Commun.*, vol. 21, no. 8, pp. 5977–5988, Aug. 2022, doi: 10.1109/TWC.2022.3144608.

[14] X. Cheng, D. Liu, C. Wang, S. Yan, and Z. Zhu, "Deep learning-based channel estimation and equalization scheme for FBMC/OQAM systems," *IEEE Wireless Commun. Lett.*, vol. 8, no. 3, pp. 881–884, Jun. 2019.

[15] Y. Zhang, J. Li, Y. Zakharov, X. Li, and J. Li, "Deep learning based underwater acoustic OFDM communications," *Appl. Acoust.*, vol. 154, pp. 53–58, Nov. 2019.

[16] X. Wei, C. Hu, and L. Dai, "Deep learning for beamspace channel estimation in millimeter-wave massive MIMO systems," *IEEE Trans. Commun.*, vol. 69, no. 1, pp. 182–193, Jan. 2021.

[17] G. Qiao, Q. Song, L. Ma, S. Liu, Z. Sun, and S. Gan, "Sparse Bayesian learning for channel estimation in time-varying underwater acoustic OFDM communication," *IEEE Access*, vol. 6, pp. 56675–56684, 2018.

[18] T. Ballal, T. Y. Al-Naffouri, and S. F. Ahmed, "Low-complexity Bayesian estimation of cluster-sparse channels," *IEEE Trans. Commun.*, vol. 63, no. 11, pp. 4159–4173, Nov. 2015.

[19] P. Chen, Y. Rong, S. Nordholm, Z. He, and A. J. Duncan, "Joint channel estimation and impulsive noise mitigation in underwater acoustic OFDM communication systems," *IEEE Trans. Wireless Commun.*, vol. 16, no. 9, pp. 6165–6178, Sep. 2017.

[20] S. Jia, S. Zou, X. Zhang, D. Tian, and L. Da, "Multi-block sparse Bayesian learning channel estimation for OFDM underwater acoustic communication based on fractional Fourier transform," *Appl. Acoust.*, vol. 192, Apr. 2022, Art. no. 108721.

[21] G. Qiao, Q. Song, L. Ma, and L. Wan, "A low-complexity orthogonal matching pursuit based channel estimation method for time-varying underwater acoustic OFDM systems," *Appl. Acoust.*, vol. 148, pp. 246–250, May 2019.

[22] S. Srivastava, P. Singh, A. K. Jagannatham, A. Karandikar, and L. Hanzo, "Bayesian learning-based doubly-selective sparse channel estimation for millimeter wave hybrid MIMO-FBMC-OQAM systems," *IEEE Trans. Commun.*, vol. 69, no. 1, pp. 529–543, Jan. 2021.

[23] M. E. Tipping and A. C. Faul, "Fast marginal likelihood maximisation for sparse Bayesian models," in *Proc. 9th Int. Workshop Artif. Intell. Statist.*, vol. 1, 2003, pp. 3–6.

[24] L. Xu, C. L. P. Chen, and R. Han, "Graph-based sparse Bayesian broad learning system for semi-supervised learning," *Inf. Sci.*, vol. 597, pp. 193–210, Jun. 2022.

[25] S. D. Babacan, R. Molina, and A. K. Katsaggelos, "Bayesian compressive sensing using Laplace priors," *IEEE Trans. Image Process.*, vol. 19, no. 1, pp. 53–63, Jan. 2010.

[26] D. Shutin, S. R. Kulkarni, and H. V. Poor, "Incremental reformulated automatic relevance determination," *IEEE Trans. Signal Process.*, vol. 60, no. 9, pp. 4977–4981, Sep. 2012.

[27] R. Mahler, *Statistical Multisource-Multitarget Information Fusion*. Norwood, MA, USA: Artech House, 2007.

[28] Y. Bar-Shalom, T. Kirubarajan, and X. R. Li, *Estimation With Applications to Tracking and Navigation*. Hoboken, NJ, USA: Wiley, 2001.

[29] R. Hou, Y. Xia, X. Zhou, and Y. Huang, "Sparse Bayesian learning for structural damage detection using expectation-maximization technique," *Struct. Control Health Monitor.*, vol. 26, no. 5, p. e2343, 2019.

SHUYANG JIA received the master's degree from the Naval University of Engineering, in 2021. He is currently pursuing the Ph.D. degree with the Naval Submarine Academy, Qingdao. His current research interests include machine learning, deep learning, and underwater communication.

SICHEN ZOU received the master's degree from Harbin Engineering University. He is currently a Researcher with the Pilot National Laboratory for Marine Science and Technology. His current research interest includes underwater communication.

XIAOCHUAN ZHANG received the master's degree from Harbin Engineering University. He is currently a Researcher with the Naval Submarine Academy. His current research interests include underwater communication and target detection.

LIANGLONG DA received the Ph.D. degree from the Naval Submarine Academy. He is currently a Professor with the Naval Submarine Academy. His current research interests include underwater communication and marine environmental effect.